Title

THE END OF INCOMPLETE FUSION AND THE DECOUPLING OF THE FIREBALL AS SEEN FROM COMPLEX FRAGMENT EMISSION

Authors

Moretto, L.G.
Bowman, D.R.
Colonna, N.

Publication Date

1989-04-01

Lawrence Berkeley Laboratory
UNIVERSITY OF CALIFORNIA

Presented at the Symposium on Nuclear Dynamics and Nuclear Assembly, Dallas, TX, April 10–14, 1989

The End of Incomplete Fusion and the Decoupling of the Fireball as Seen from Complex Fragment Emission

L.G. Moretto, D.R. Bowman, N. Colonna, and G.J. Wozniak

April 1989

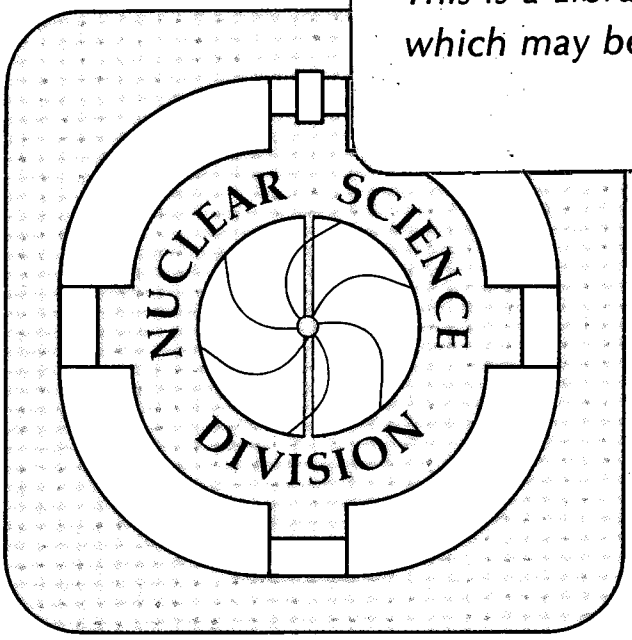

Prepared for the U.S. Department of Energy under Contract Number DE-AC03-76SF00098.

DISCLAIMER

The End of Incomplete Fusion and the Decoupling of the Fireball As Seen From Complex Fragment Emission

L. G. Moretto, D. R. Bowman, N. Colonna, and G. J. Wozniak

Nuclear Science Division, Lawrence Berkeley Laboratory, 1 Cyclotron Rd., Berkeley, California 94720, USA

ABSTRACT

The incomplete fusion process is affected by the entrance channel asymmetry as well as by the bombarding energy. In the first part of the paper, the role of entrance channel mass asymmetry is explored by characterizing the resulting complex fragment sources in terms of their velocity, charge and excitation energy. In the second part evidence is given about the possible demise of incomplete fusion and the onset of the fireball regime from the anomalous charge and angular distributions of the emitted complex fragments. Complete ternary events are analyzed and discussed in terms of sequential binary decay.

1. INTRODUCTION

At the lowest bombarding energies, heavy ion collisions give rise to either quasi/deep-inelastic reactions or to complete fusion. As the energy is increased, incomplete fusion takes over. In this process only a part of the lighter partner fuses, while the other is found as a rather cold spectator. At even higher energies, incomplete fission is substituted by the so-called fireball regime. In this case the overlapping regions of the target and projectile form an interaction zone (fireball) that detaches itself from the target and projectile remnants. A simple explanation of this scenario can be given in terms of a geometric model.[1] For any given impact parameter one can imagine a clean cut produced by one partner into the other. The energy necessary for this cut can be estimated from the additional surface created by such a cut. This energy, plus two-body kinematics defines a threshold bombarding energy for incomplete fusion. The cut of the heavy into the light partner produces a smaller surface than the alternative cut by the light fragment into the heavy fragment. Therefore, the threshold for the former process should be the lower one and one should observe (and one does!) a predominance of reactions in which the light partner suffers the cut and the heavy partner picks up the piece.

While the thresholds for the onset of incomplete fusion can be defined from the energy of the cut and from kinematics, the threshold for the decoupling of the fireball from the heavy partner cannot be defined so simply, but requires some understanding of the dynamics.

From this simple analysis, one learns that the region of existence of incomplete fusion is defined not only by the bombarding energy but also by the impact parameter and by the geometrical sizes of the partners. In other words, the entrance channel mass asymmetry should be just as important as the bombarding energy in defining the boundaries of incomplete fusion.

A large amount of information, though still incompletely digested, is available to define the onset of incomplete fusion. Almost no information is available on the termination of incomplete fusion and the onset of the fireball formation.

Complex fragments produced in the statistical decay of the fusion products provide an especially good and rather general tool for the study of incomplete fusion. In this paper we illustrate the role of the entrance-channel mass asymmetry at low bombarding energy and the onset of the fireball formation at high energy through the observation of complex fragments emitted by the fusion products.

2. INCOMPLETE FUSION AND ENTRANCE-CHANNEL MASS ASYMMETRY

Studies[2-11] with very asymmetric target-projectile systems have led to the identification of the compound nucleus as an important source of complex fragments formed in binary decays at all exit channel asymmetries. These compound nuclei are formed in complete or incomplete fusion processes, depending on the entrance channel asymmetry and on the bombarding energy. Simple source patterns in the $v_{\parallel}$ - $v_{\perp}$ plane are observed at low energy because of the dominance of complete fusion.[5-7] At higher energies[9-11], when incomplete fusion sets in, the source patterns still remain simple. The narrow range of source velocities responsible for this simplicity is results from the interplay between incomplete fusion and complex-fragment decay probability, through their dependence upon impact parameter.[11]

This simple source pattern disappears in more symmetric systems. This may be caused by the increased range of impact parameters leading to a broad range of incomplete-fusion products and to a corresponding broad range of source velocities. However, the lessons learned from the very asymmetric systems have helped unravel the puzzle.

As already hinted above, it turns out that the only substantive change occuring in

more symmetric systems is the formation of a continuous range of sources associated with the full range of incomplete fusion processes. These sources have a continuum of velocities, total masses, and excitation energies, but in all other respects they resemble the fusion products formed in more asymmetric systems, and decay in a similar way. This has been shown in the reaction $^{139}La + ^{64}Ni$ at 18 A MeV, for which the distribution of source velocities has been determined, their mass and excitation energy has been established, and the consistency of the missing charge with evaporation from the hot fragments has been demonstrated.[12]

In Fig. 1b the cross section $\partial^2\sigma/\partial v_{||}\partial v_{\perp}$ in the $v_{||}$ - $v_{\perp}$ plane is shown for binary coincidences in which one fragment has the atomic number Z = 30. In this display, one observes an elliptical pattern stretched along the beam direction. Although a high degree of kinetic energy relaxation can be inferred, it is not possible to associate these events with a single source. For comparison, a more asymmetric reaction like $^{139}La + ^{12}C$ (see Fig. 1a) shows a sharp isotropic Coulomb circle indicating the presence of a single source with a well defined velocity. Also the Z_1-Z_2 correlation diagram for the $^{139}La + ^{64}Ni$ reaction (Fig. 1g) is very broad, whereas that for the $^{139}La + ^{12}C$ reaction (Fig. 1f) is much narrower.

The cause of these "anomalous" features becomes apparent when the velocity spectrum of the centers of mass of the coincident fragments is determined. This spectrum is shown in Fig. 2 for three reactions: 18 A MeV $^{139}La + ^{12}C$, ^{27}Al and ^{64}Ni. For the very asymmetric $^{139}La + ^{12}C$, ^{27}Al systems, the center-of-mass velocity spectra show single sharp peaks. These peaks correspond to the velocities of the centers-of-mass of the entire system and indicate the absence of a substantial third body. The total relaxation of the kinetic energies, mass and angular distributions allows one to attribute these peaks to a complete fusion process.

For the more symmetric $^{139}La + ^{64}Ni$ reaction, one observes a similar peak, that can also be attributed to complete fusion, plus an additional shoulder that stretches out to velocities approaching that of the projectile. This high velocity shoulder indicates the presence of a substantial third body (target-like spectator) associated with a continuum of incomplete fusion processes extending over the entire allowed mass range.

Of course, caution must be exercised in interpreting this curve as the "true" distribution in source velocities. On the one hand, the peak can contain all kinds of two body decays, in particular deep-inelastic decay. On the other, the measured distribution may be biased (though not seriously) by the coincidence efficiency of the apparatus. Furthermore, the velocity spectrum is broadened by light particle evaporation, which may

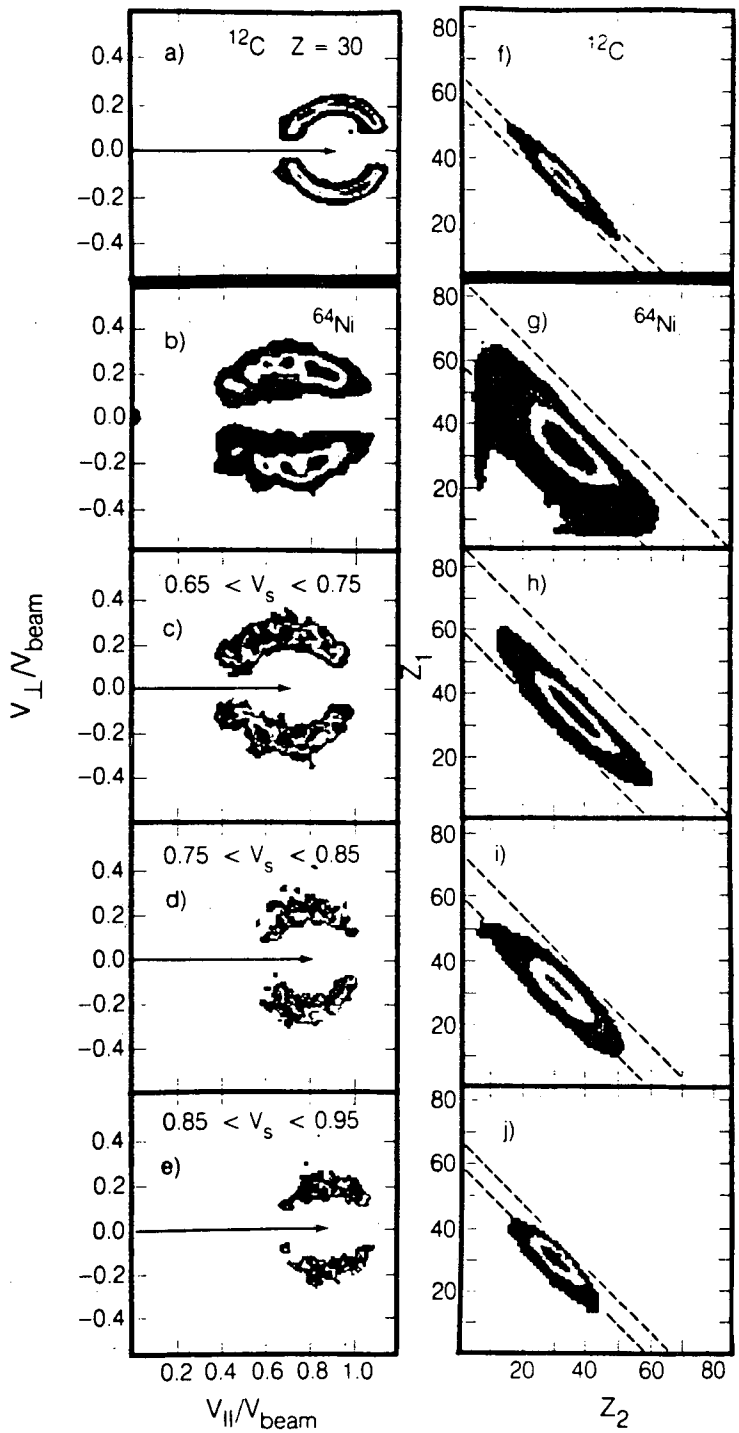

Fig. 1 Contour diagrams of invariant cross section in the V_{II} - $V_\perp$ plane (left column) and Z_1 - Z_2 (right column) for Z = 30 fragments from the 18 A MeV ^{139}La + ^{12}C reaction (first row) and for the 18 A MeV ^{139}La + ^{64}Ni reaction. Various gating conditions on the source velocity are indicated to the left of each row. The horizontal arrows indicate the magnitude of the source velocity and the diagonal dashed lines indicate the atomic numbers of the projectile and of the fused system as inferred from the source velocity.

either precede or follow complex fragment decay.

Despite these possible biases, the measured source velocity distribution can be used to unravel the complexity of the $^{139}La + ^{64}Ni$ reaction by selecting events with well defined source velocities. For example, in Fig. 1(c, d, & e), the velocity plots for Z = 30 are gated on three different velocity bins, centered on the velocities corresponding to complete fusion, 50% fusion and 25% fusion. These three velocity plots now display isotropic circular patterns similar to the Coulomb circles seen in the very asymmetric systems, but with their centers progressively shifted towards higher values of $v_{||}$. There is also a striking decrease in the radii of these Coulomb circles with increasing source velocity. These correlations occur since, as the projectile picks up more mass from the target, its velocity decreases correspondingly. The complex fragment is thus emitted from a heavier and slower source. In addition, as the total charge of the source decreases, the Coulomb velocity associated with a fixed fragment Z value decreases, because the splitting becomes more symmetric.

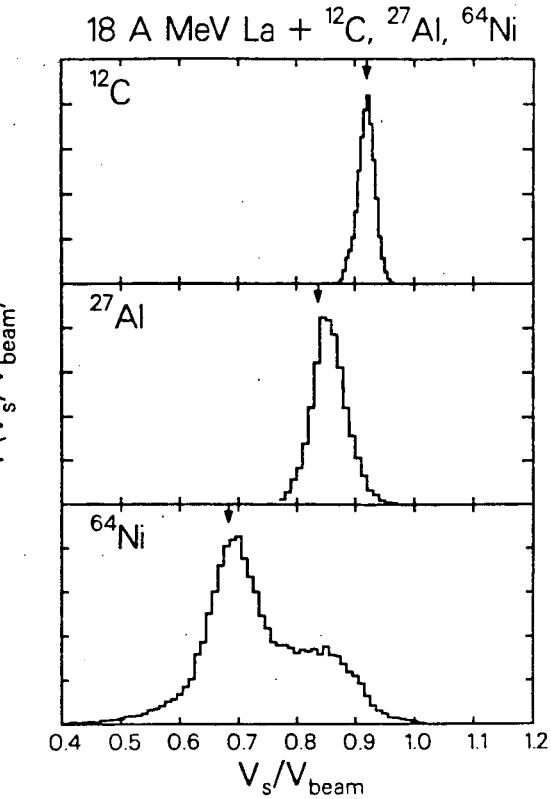

Fig. 2 Source velocity distributions for the 18 A MeV $^{139}La + ^{12}C$, ^{27}Al, ^{64}Ni reactions as extracted from the binary coincidences (see text). The vertical arrows indicate the velocities corresponding to complete fusion for the three reactions.

The ungated Z_1-Z_2 correlation diagram as well as those gated on the same velocity bins are also shown in Fig. 1. The ungated diagram (see Fig. 1g) shows a broad distribution in the total charge of the source due to the extended range of incomplete fusion. By restricting the source velocity, this broad distribution is decomposed into three narrower correlation diagrams (see Fig. 1h, i, j), with the characteristic pattern observed for very asymmetric systems like $^{139}La + ^{12}C$ (see Fig. 1f). As the source velocity increases, the diagonal pattern shifts from larger to smaller total Z values. The greatest average sum of the fragment atomic numbers $\langle Z_1 + Z_2 \rangle$ occurs for the complete fusion velocity. The quantity $\langle Z_1 + Z_2 \rangle$ decreases with increasing source velocity,

which corresponds to progressively less extensive fusion of the target with the projectile. Thus, the broad ungated correlation diagram observed in Fig. 1g, can be decomposed into a series of narrower patterns, by setting gates on the source velocity.

The observed atomic numbers of the coincident fragments are those resulting after evaporation from either the hot compound nucleus, or the hot primary fragments resulting from its binary decay. It would be useful to obtain information on their primary atomic numbers. One can estimate the total primary charge of the incomplete fusion product from the corresponding source velocity, namely:

$$Z_{IF} \cong Z_P V_P / V_{IF} \cdot \qquad (1)$$

Similarly, one can estimate the excitation energy of the incomplete fusion product:

$$E_x(IF) \cong E_x(CF) \frac{V_P - V_{IF}}{V_P - V_C} . \qquad (2)$$

For complete fusion, one obtains $E_x \sim 800$ MeV for the compound nucleus ^{205}At, which corresponds to 4 MeV/nucleon and a temperature of 6.5 MeV. While higher temperatures have been advocated from spectral slopes or particle multiplicities, this may well be the highest temperature that can be firmly associated with a well characterized system.

One should be aware that light particle evaporation causes some uncertainty in these estimated quantities. With this caution in mind, one can plot the <u>difference</u> between the <u>estimated</u> primary charge and the <u>measured</u> average secondary charge as a function of the estimated excitation energy (see Fig. 3). The approximate linearity of the plot is consistent with the evaporation hypothesis. A more quantitative check can be made by assuming that the binary decay occurs first, and that all of the remaining excitation energy is disposed of by

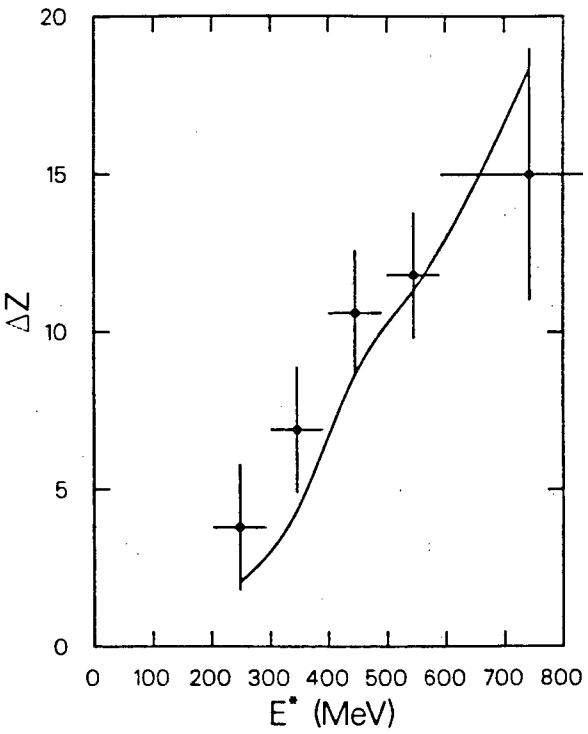

Fig. 3 The measured evaporated charge (dots) plotted versus the excitation energy determined from the source velocities for the 18 A MeV $^{139}La + ^{64}Ni$ reaction. The horizontal and vertical bars on each data point reflect the width of the bin in the source velocity from which the primary charge and the excitation energy of the incomplete fusion product was extracted. The solid line was calculated with the evaporation code PACE (see text).

evaporation from the two fragments.

The results obtained from the evaporation code PACE are shown in the same figure. Given the very rough assumptions of equations 1 & 2 and the crude estimate of the angular momentum of the fragments, the agreement between the data and the calculations is quite satisfactory.

In light of the above discussion, the 18 A MeV $^{139}La + ^{64}Ni$ reaction can be described as follows: 1) The events associated with the "complete fusion peak" arise from either compound nucleus binary decay of the complete fusion object, or from quasifission binary decay, or, possibly, from (quasi) deep inelastic reactions. 2) The events associated with the higher velocity components are essentially ternary incomplete fusion events. The target-like spectator, observable in singles[6-11] as part of the low velocity "big foot" is not detected in coincidence. The forward moving incomplete fusion products, whose masses are smaller the faster their velocities, give rise to the observed continuum of complex fragment sources. 3) If the incomplete fusion product undergoes a binary decay, this continuum can be analyzed by reconstructing the source velocity from the two coincident heavy fragments. It is clear that other more symmetric systems could be studied in a similar fashion.

3. BOMBARDING ENERGY DEPENDENCE OF INCOMPLETE FUSION

The pattern of incomplete fusion followed by compound nucleus emission of complex fragments, observed over a large range of bombarding energies, should terminate when the bombarding energy is sufficiently large. In the same way as the non-occluded part of the lighter partner detaches to form a spectator in incomplete fusion, so should the non-occluded part of the heavy partner detach eventually to form another spectator. The overlapping parts should form a hot blob (the fireball[13]) distinct from the two spectators.

At what energy should this decoupling of the fireball from the heavy reaction partner occur? An estimate from an incomplete fusion model for the reaction $^{139}La + ^{12}C$ suggests that the decoupling ought to occur aroung 80 A MeV.[1]

Dramatic changes and novel features have been observed in the reaction $^{139}La + ^{12}C$ at 80 & 100 A MeV that may be related to the incipient decoupling of the fireball. In this reaction the appearance of well defined Coulomb rings at all atomic numbers (see Fig. 4) indicates the presence of a fairly sharp source and the predominance of binary decay. However, the distributions along the Coulomb rings are not isotropic. They are

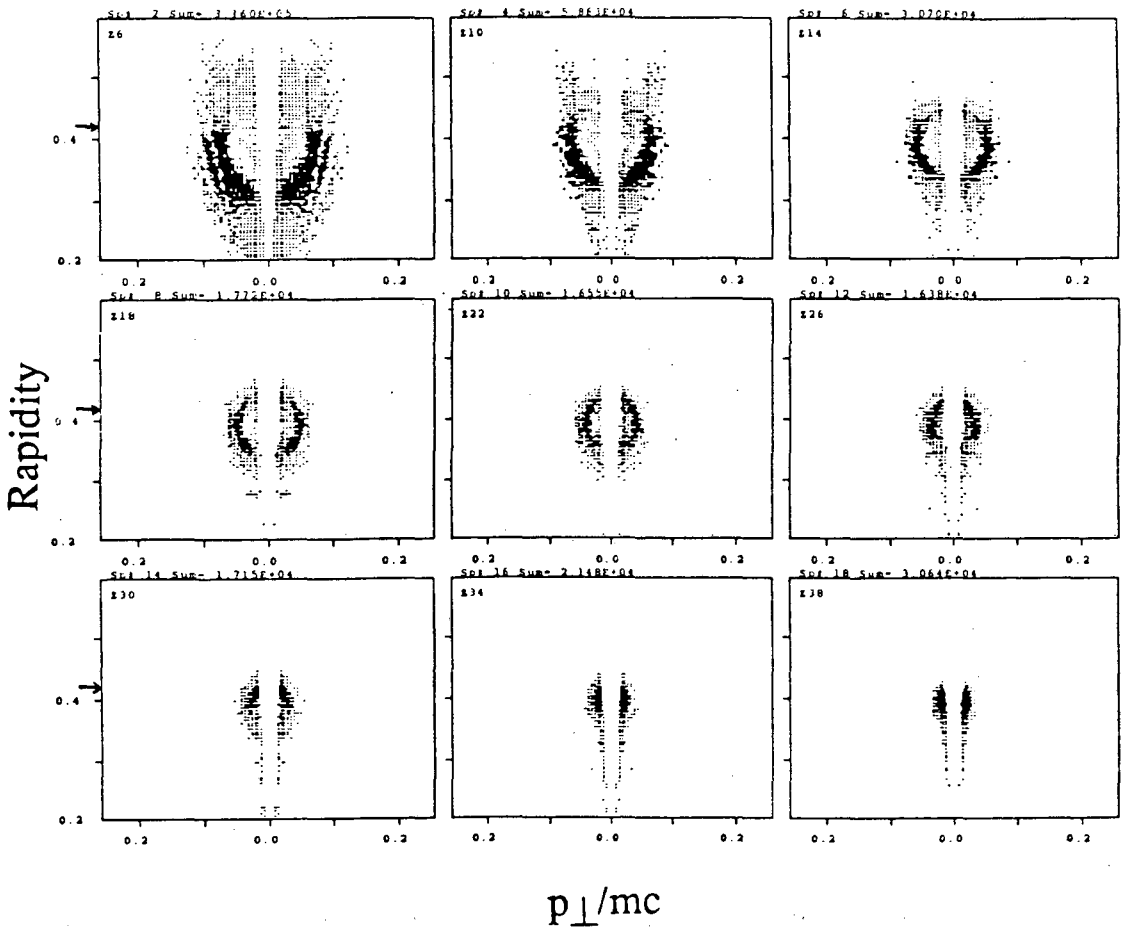

Fig. 4 The invariant cross sections in rapidity vs. transverse momentum space $d^2\sigma/dy\ d(p_\perp/mc)$ for the 80 A MeV $^{139}La + ^{12}C$ reaction gated on the indicated Z-values. The beam direction is vertical. The distributions are centered near the beam rapidity (arrows). Events populate mainly the Coulomb rings for all of these Z-values. With increasing Z-value, the fragment angular distributions in the source frame evolve from backward- to slightly side- and then forward-peaked.

backward peaked from $6 \leq Z \leq 18$, side peaked from $19 \leq Z \leq 25$ and forward peaked for $Z > 26$, the rather broad peak moving continuously from one extreme to the other as shown in Fig. 5. This behavior is quite new. For instance, in the same reaction at 18 A MeV, the backward peaking is confined $Z < 8$ and the forward peaking to $Z > 40$, while a rigorously flat distribution is observed for all of the intermediate Z-values. At 50 A MeV, the products of $22 \leq Z \leq 35$ are each forward/backward symmetric. This

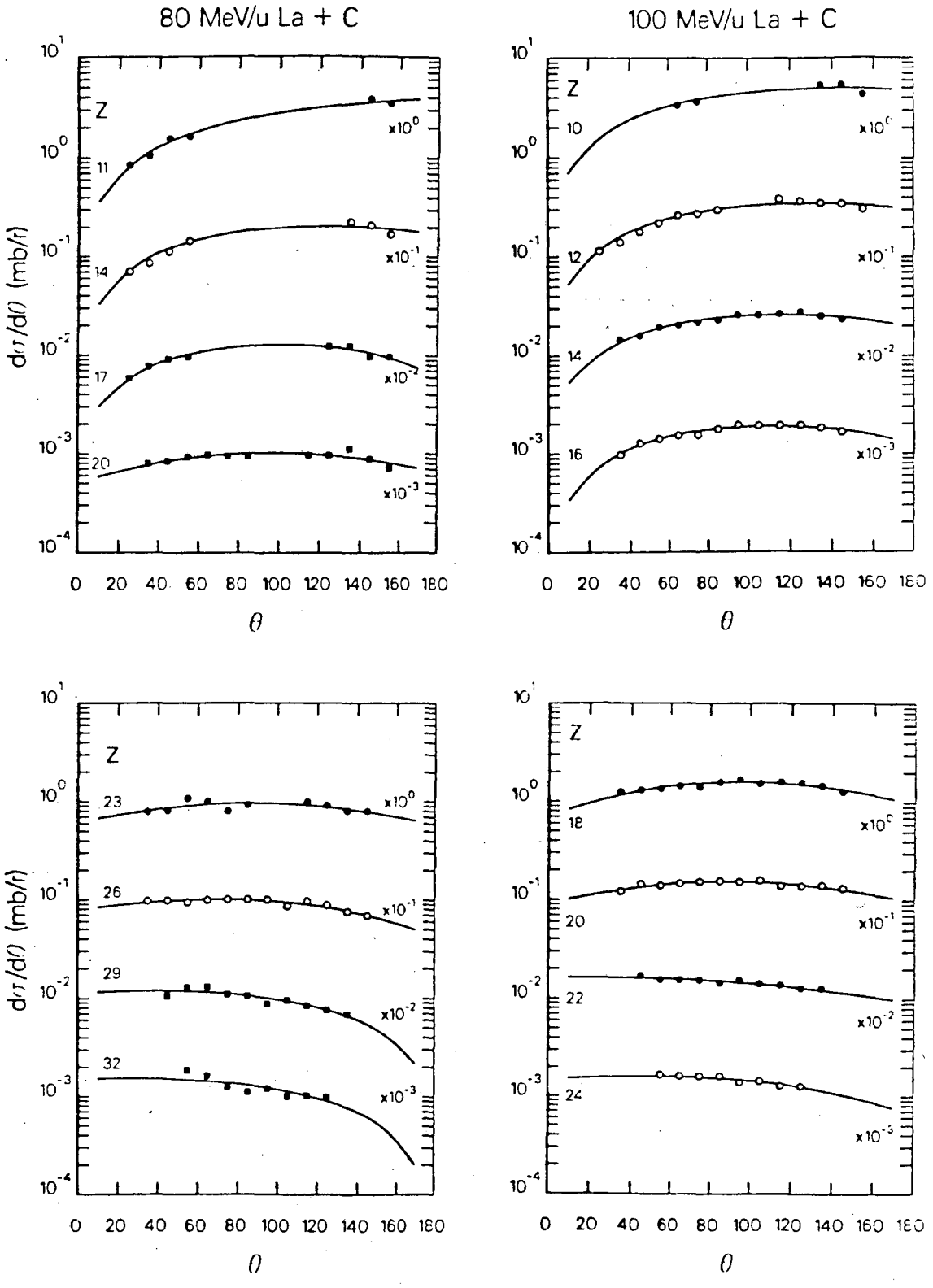

Fig. 5 Angular distributions in the c.m. system for the representative Z-values from the 80 & 100 A MeV $^{139}La + ^{12}C$ reactions.

perturbation in the angular distributions seems to be dynamical in origin. It is possible that the nascent fireball, still attached to the heavy partner tries to detach itself by stretching out toward the light partner spectator. The decay may then occur from this stretched configuration giving rise to a rather light fragment pointing toward the backward hemisphere where the light spectator is located. At much larger energies, where the decoupling of the fireball is complete and the fragments are emitted from the target spectator, the angular distributions are very nearly isotropic.[14]

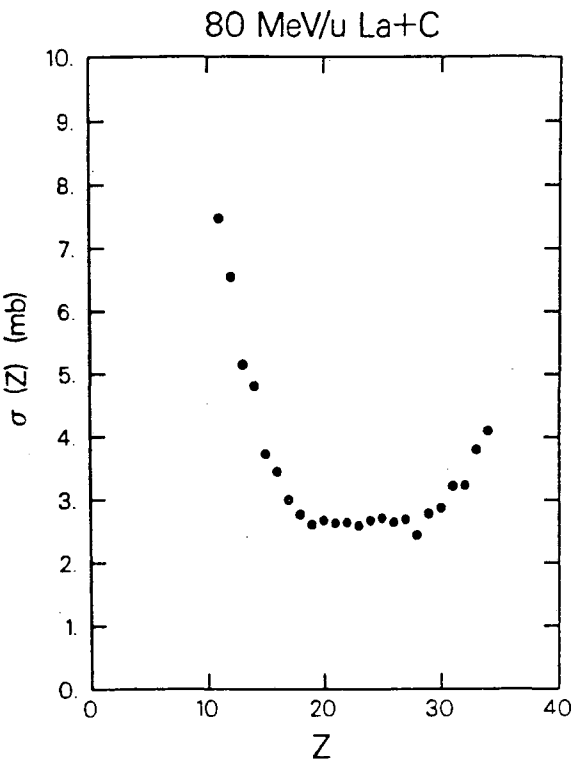

Fig. 6 Integrated charge distributions for the 80 A MeV $^{139}La + ^{12}C$ reaction.

The total cross sections as a function of atomic number shown in Fig. 6 are also rather peculiar. The Z distribution is U shaped and shows no hint of a symmetric peak, while at lower energies the symmetric peak is most prominent. Of course an increase in temperature is expected to flatten out the distribution and to reduce the sharpness of the symmetric peak. However, here the central peak is totally absent and the cross section increases dramatically for $Z < 20$. This distribution may indicate the presence of dynamical effects. In particular, the fragments with $Z < 20$ may very well be associated with the breaking off of the stretched out portion of the system associated with the nascent fireball.

The study of binary and ternary coincidences is also very instructive. The center-of-mass rapidities extracted for both classes of events are shown in Fig. 7. The two distributions are essentially identical and correspond to an average momentum transfer of about 50%. This identity suggests that both binary and ternary events arise from the same source. This is made even more likely by the spectra of the total charge for both binary and ternary events at two bombarding energies shown Fig. 7. The identity of these two distributions is striking and in conjunction with the identity of center-of-mass rapidities leaves little doubt on the uniqueness of the source.

The charge distribution of ternary events can be best appreciated by means of a

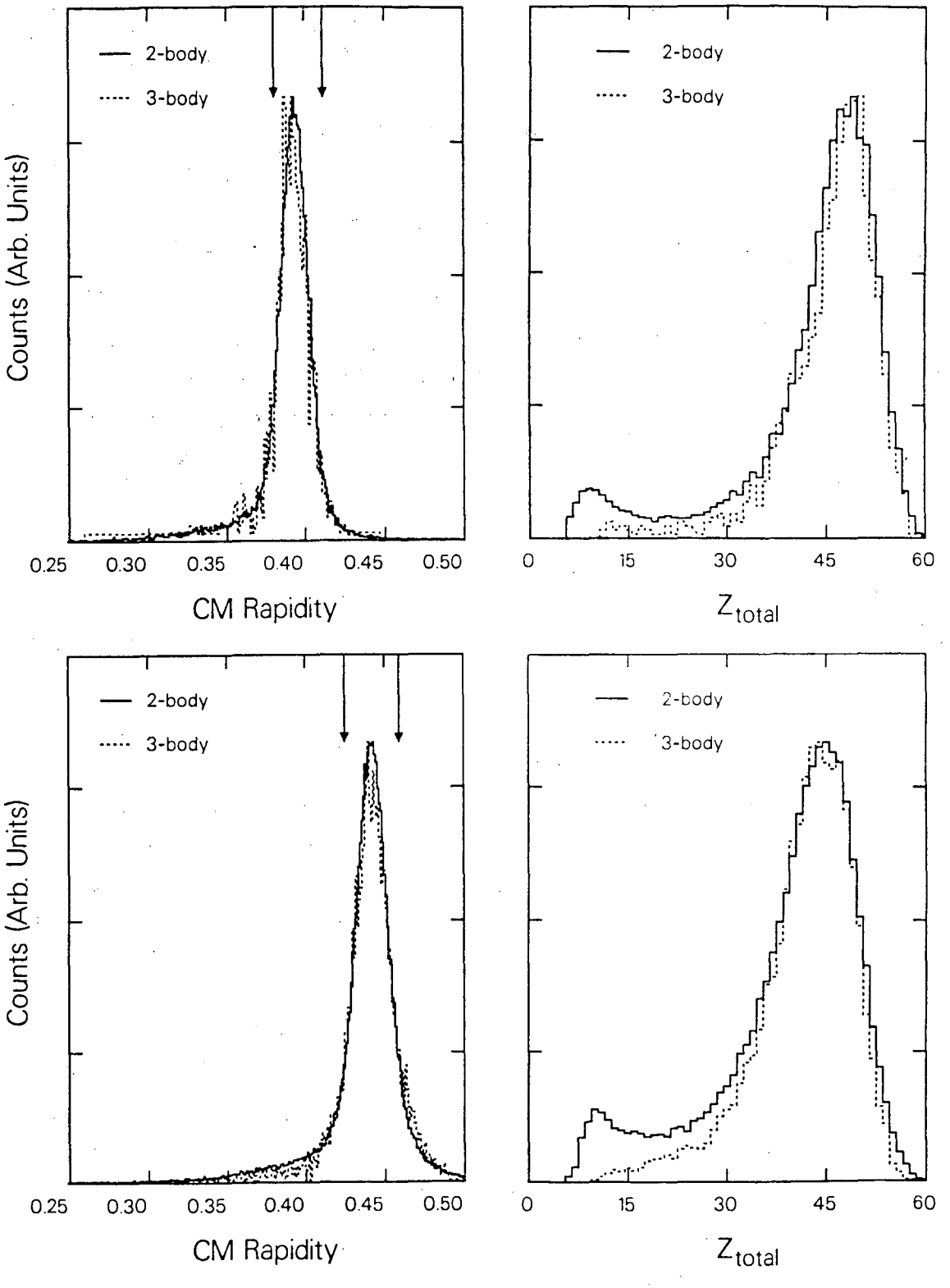

Fig. 7 The extracted rapidity (left column) and summed charge distributions (right column) for binary (solid curve) and ternary (dotted curve) events from the 80 & 100 A MeV $^{139}La + ^{12}C$ reactions.

Dalitz plot. In Fig. 8 the plot for ternary coincidences is shown. It has been obtained by gating on the peak of the sum charge distribution, $45 \leq Z_{total} < 55$, and by plotting Z_1/Z_{total} vs. Z_2/Z_{total} vs. Z_3/Z_{total}. (In a triangular Dalitz plot one would require $Z_1 + Z_2 + Z_3$ = constant). The band of high cross section along the edges of the triangle means that one of the three fragments is always relatively small. In fact, the cross section has a minimum in the center of the triangle which corresponds to three equal fragments. However, if one looks at the distribution of the remaining two fragments along the band of high cross section parallel to one side, one observes two complementary wings at large asymmetries and a symmetric peak. The latter distribution is quite familiar and expected for the decay of a system slightly above the Businaro-Gallone point. Thus it is very tempting to assume that the ternary events arise from two sequential binary decays. The first decay may be a non-statistical decay

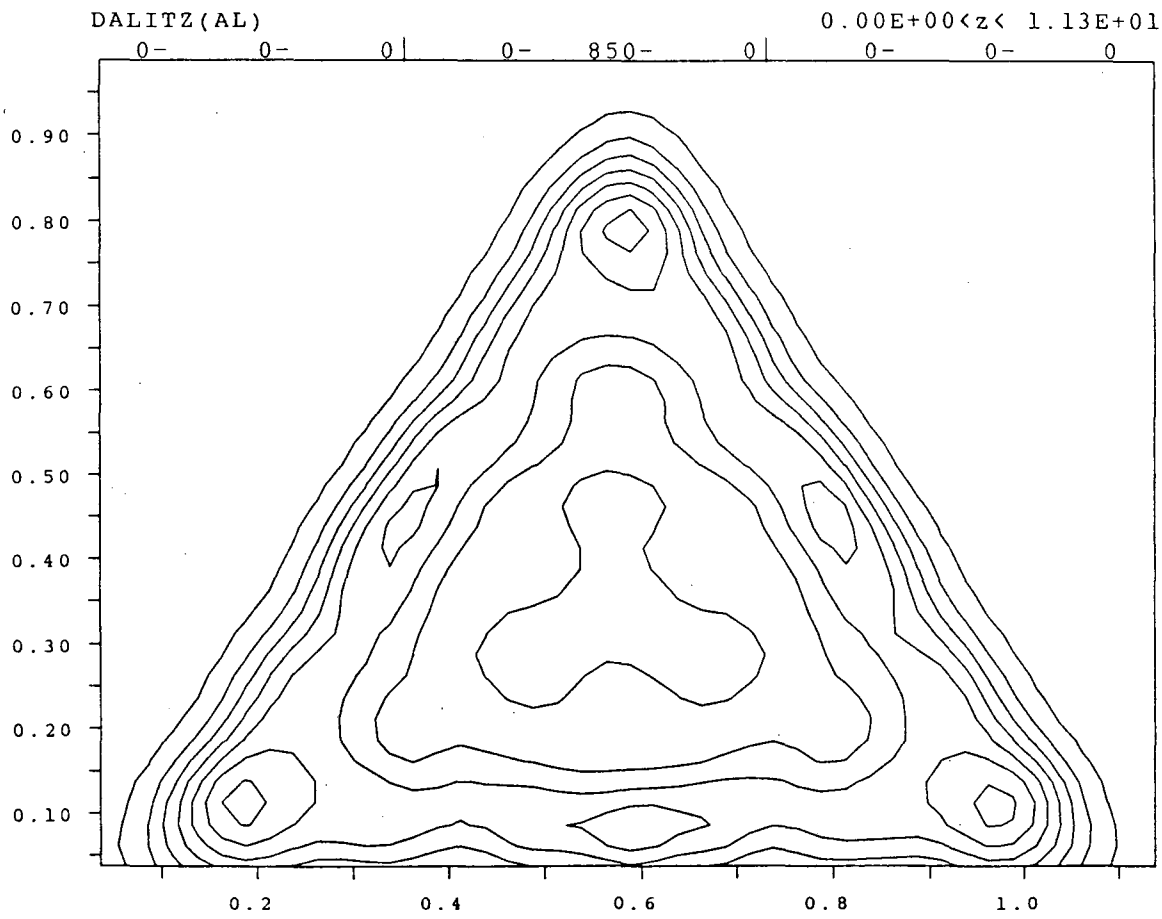

Fig. 8 Dalitz plot of 3-body events (Z_1-Z_2-Z_3) for the 80 A MeV $^{139}La + ^{12}C$ reaction.

producing a very asymmetric split as discussed above for the total Z distribution. The heavy fragment then proceeds to decay in a more statistical fashion giving rise to the characteristic asymmetric wings and to a symmetric peak.

In conclusion this reaction shows a distinct departure from the features observed at lower energy. While both binary and ternary events appear to arise from the decay of the same source, the angular distribution of the fragments as well as the charge distributions of binary and ternary events seem to indicate deviations from the statistical model. The stretched and stressed configurations of the incomplete fusion product due to the incipient decoupling of the fireball may be responsible for the observed dynamic effects.

Acknowledgements

This work was supported by the Director, Office of Energy Research, Office of High Energy and Nuclear Physics, Division of Nuclear Physics, of the U.S. Department of Energy under Contract DE-AC03-76SF00098.

References

1. Moretto, L. G. and Bowman, D. R., Proc. of the XXIV Int'l Winter Meeting on Nucl. Phys., Bormio, Italy, Jan. 20 - 25, 1986, Ricerca Scientifica ed Educazione Permanente, Suppl. N. 49, 126 (1986).
2. Moretto, L. G. and Wozniak, G. J., Prog. in Part. & Nucl. Phys. 21, 401 (1988).
3. Sobotka, L. G. et al., Phys. Rev. Lett. 51, 2187 (1983).
4. McMahan, M. A. et al., Phys. Rev. Lett. 54, 1995 (1985).
5. Sobotka, L. G. et al., Phys. Rev. Lett. 53, 2004 (1984).
6. Charity, R. J. et al., Nucl. Phys. A483, 371 (1988).
7. Han, H. et al., Nucl. Phys. A492, 138 (1989).
8. Plagnol, E. et al., LBL-25742, Phys. Lett. B, in press, (1989).
9. Charity, R. J. et al., Phys. Rev. Lett. 56, 1354 (1986).
10. Bowman, D. R. et al., Phys. Lett. B189, 282 (1987).
11. Charity, R. J. et al., Nucl. Phys. A476, 516 (1988).
12. Colonna, N. et al., Phys. Rev. Lett. (in press), LBL-26459 (1989).
13. Bowman, J. D., Swiatecki, W. J. and Tsang, C. F., LBL-2908.
14. Warwick, A. I. et al., Phys. Rev. C27 1083 (1983), and references therein.

LAWRENCE BERKELEY LABORATORY
TECHNICAL INFORMATION DEPARTMENT
1 CYCLOTRON ROAD
BERKELEY, CALIFORNIA 94720